Numerical Studies on the Influence of Step-Like Surface Irregularities on the Development of Tollmien-Schlichting Waves

Juan Alberto Franco and Stefan Hein

Abstract The effect of a single step-like surface irregularity on the spatial development of Tollmien-Schlichting (TS) waves is investigated by the recently developed Adaptive Harmonic Linearized Navier-Stokes (AHLNS) methodology. The steps considered in the present work, forward- and backward-facing steps (FFS & BFS), are varied not only in height but also in shape (rectangular and rounded). This work is motivated by the growing interest in the aeronautical industry on the effect of surface irregularities on the location of laminar-turbulent transition. The main contribution of this paper is to present, for fixed flow conditions, the combined influence of the height and shape of step-like irregularities on the expected transition location. A second motivation of this paper is to demonstrate the AHLNS methodology used in the course of this investigation as a perfectly suited stability analysis tool for performing numerical studies on the effect of surface irregularities on the spatial development of traveling instabilities with a relatively moderate computational effort.

1 Introduction

One of the key areas for present and future aircraft design is to achieve a significant drag reduction by delaying the transition of the incoming free-stream air from laminar to turbulent state. The presence of surface irregularities like steps, gaps, humps, etc. introduces regions of localized strong streamwise gradients in the base flow quantities. TS waves may lead to the onset of laminar-turbulent transition and therefore, it becomes critical to correctly model their interaction with the above mentioned surface irregularities.

J. A. Franco (✉) · S. Hein
DLR - German Aerospace Center, Bunsenstrasse 10, 37073 Göttingen, Germany
e-mail: Juan.Franco@dlr.de

S. Hein
e-mail: Stefan.Hein@dlr.de

J. A. Franco
UPM - Universidad Politécnica de Madrid, Madrid, Spain

S. Sherwin et al. (eds.), *IUTAM Laminar-Turbulent Transition*, IUTAM Bookseries 38,
https://doi.org/10.1007/978-3-030-67902-6_64

Techniques like Parabolized Stability Equations (PSE) are not suited for boundary-layer instability analysis in the vicinity of those surface irregularities: its formulation assumes that streamwise variations of base flow and disturbances quantities are small (compared to surface-normal variations), allowing a marching procedure for their resolution. Moreover, PSE is unable to resolve the very short-scale streamwise variations in the base flow due to its step size limitations. On the other hand, techniques like Linearized Navier-Stokes (LNS), Harmonic LNS (HLNS) and Direct Numerical Simulation (DNS) do not impose any assumption regarding the nature of the convective instabilities in streamwise direction. This fact implies that the required numerical resources increase significantly. Alternatively, the Adaptive Harmonic LNS (AHLNS) equations can also handle these large streamwise gradients by using a fully-elliptic system of equations (similar to DNS). The AHLNS formulation assumes a wave-like character of the instabilities (as in PSE), leading to a significant reduction in the number of streamwise grid points required compared with LNS, HLNS or DNS computations.

The effect of steps on the onset of laminar-turbulent transition has been extensively studied, both numerically and experimentally. One of the first attempts was done by Nenni and Gluyas [1], who provide a critical Reynolds number based on the step height (for rectangular FFS & BFS). Smooth BFS steps were considered by Ragab and Nayfeh [2] using LST (Local Stability Theory). Recently, Edelmann [3] studied the effect of rectangular FFS by means of DNS. He found that there was a good agreement between DNS and LST, assuming that a small region around the step is omitted from the LST computations.

The present paper provides a systematic study of the effect of a single step (FFS and BFS) on the spatial development of TS waves in a compressible subsonic flow. The height and shape have been varied in order to provide a clearer understanding how these parameters influence the base flow and the linear growth of the oncoming TS waves. A similar work about the effect of a single hump on laminar-turbulent transition has been recently published by Franco et al. [4]. To the authors' knowledge, there is no similar work published regarding the influence of a single step.

2 Problem Description

2.1 Setup

We study numerically the effect of a single step on boundary-layer transition of a two-dimensional laminar flow on a flat plate. Figure 1 shows schematically the computational domain used in the present study, including the type of boundary conditions imposed for computing the laminar base flow. All dimensional quantities are marked with an asterisk *. The free-stream Mach number Ma_∞ is set to 0.5 for all cases. The shape of the step is defined by the expression

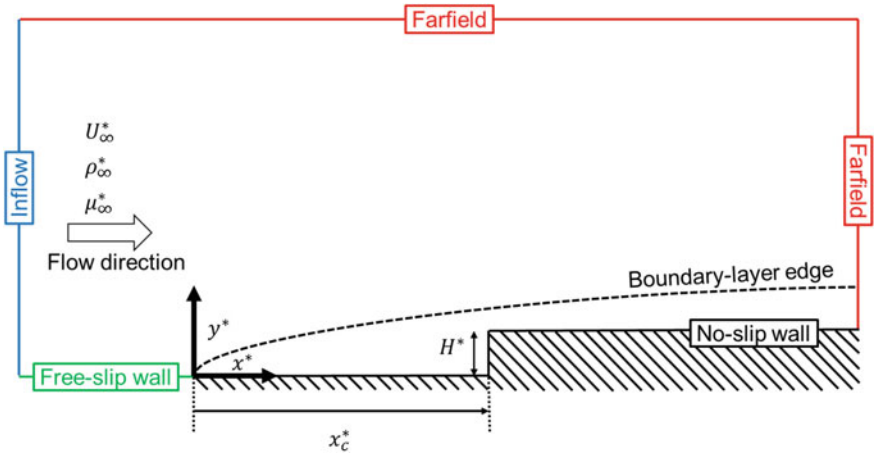

Fig. 1 Schematic representation of the computational domain defined for the present study. The labels at the edges of the domain indicate the type of boundary conditions used for the base flow computations

$$y^* = \frac{H^*}{2}\left(1 + \mathrm{erf}\left(\frac{1}{C}\frac{x^* - x^*_c}{\delta^*}\right)\right), \tag{1}$$

where the parameter H^* indicates the height of the step (positive for FFS and negative for BFS). The center of the step is placed at x^*_c. The geometrical parameter C defines the shape of the step. The rectangular shape can be considered the limiting case when $C \to 0$. Geometrical quantities are nondimensionalized with δ^* (the compressible boundary-layer displacement thickness at the x^*_c position for a flat plate at zero pressure gradient (ZPG)). The Reynolds number based on δ^* is defined as $Re_{\delta^*} = \frac{\rho^*_\infty U^*_\infty \delta^*}{\mu^*_\infty}$, where ρ^*_∞, u^*_∞ and μ^*_∞ denotes the density, velocity and dynamic viscosity at the boundary-layer edge, respectively. In the present study, the value of Re_{δ^*} at the step location x^*_c is fixed to 1823. We will consider three values for the geometric parameter C: 10, 50 and the rectangular-shaped case r, i.e. $C \to 0$. For the nondimensional height H, six values will be examined here: $\pm$ 0.4 (*small*), $\pm$ 0.8 (*medium*) and $\pm$ 1.2 (*large*). The combination of parameters H and C gives a total of 18 types of surface irregularities, which are summarized in Table 1.

2.2 AHLNS Equations

The boundary-layer instability analysis of the above mentioned configurations will be done using the Adaptive Harmonic Linearized Navier Stokes (AHLNS) equations [5] in combination with linear PSE [6], following a multi-zonal approach as described in Fig. 2. Here, a brief introduction to the AHLNS methodology is given. For a detailed

Table 1 Values of the nondimensional parameters H and C considered in the present study. The case $C = r$ refers to the rectangular-shaped step. The maximum slope of the wall is also included

Case name	H	C	Max. slope	Case name	H	C	Max. slope
FFS_H04_C50	0.4	50	0.26°	BFS_H04_C50	−0.4	50	−0.26°
FFS_H04_C10	0.4	10	1.29°	BFS_H04_C10	−0.4	10	−1.29°
FFS_H04_r	0.4	r	90°	BFS_H04_r	−0.4	r	−90°
FFS_H08_C50	0.8	50	0.52°	BFS_H08_C50	−0.8	50	−0.52°
FFS_H08_C10	0.8	10	2.58°	BFS_H08_C10	−0.8	10	−2.58°
FFS_H08_r	0.8	r	90°	BFS_H08_r	−0.8	r	−90°
FFS_H12_C50	1.2	50	0.78°	BFS_H12_C50	−1.2	50	−0.78°
FFS_H12_C10	1.2	10	3.87°	BFS_H12_C10	−1.2	10	−3.87°
FFS_H12_r	1.2	r	90°	BFS_H12_r	−1.2	r	−90°

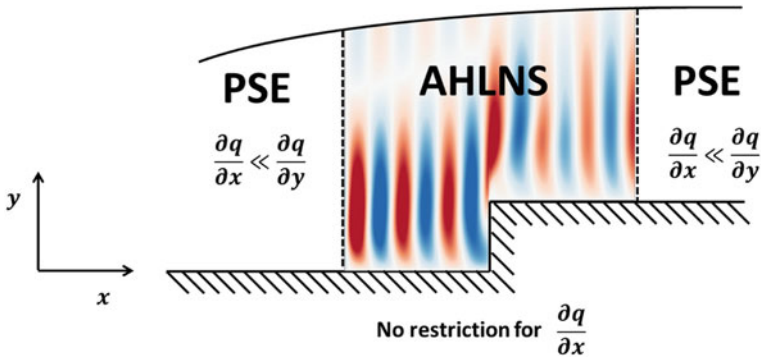

Fig. 2 Sketch of the multi-zonal technique for boundary-layer instability analysis in the presence of surface irregularities. The vertical dashed lines represent the inflow and outflow locations for AHLNS computations. A TS wave of reduced frequency $F = 20$ is depicted (case *FFS_H08_r*)

description of this methodology, the readers are referred to Franco and Hein [5]. For a complete explanation about the PSE methodology, the readers are referred to Hein et al. [6].

The AHLNS equations are obtained from the compressible Navier-Stokes (NS) equations linearized for small disturbances. All flow and material quantities $\mathbf{q}$ are decomposed into a steady base flow $\bar{\mathbf{q}}$ plus an unsteady disturbance flow component $\tilde{\mathbf{q}}$, i.e. $\mathbf{q}(\mathbf{x}, t) = \bar{\mathbf{q}}(\mathbf{x}) + \varepsilon\tilde{\mathbf{q}}(\mathbf{x}, t)$, with $\varepsilon \ll 1$. Here, t represents time. This flow decomposition is introduced into the NS equations, then the base state solution is subtracted and products of disturbance quantities are neglected. To further simplify the analysis, it is assumed that the base flow is homogeneous in spanwise z direction. Moreover, disturbances are assumed to be periodic in time t and in spanwise z direction. The adaptive approach is introduced here: the disturbance flow variables are divided into an amplitude function and a suitable, iteratively updated

wave function, i.e. $\tilde{\mathbf{q}}(x, y, z, t) = \hat{\mathbf{q}}(x, y)e^{i\Theta}$, where the wave function is defined as $\Theta = \int \alpha(x)dx + \beta z - \omega t$. The major advantage of the adaptive approach is that it exploits the *wave-like* character of the convective instabilities in a similar fashion as in the PSE method. However, unlike to the PSE approach [6], the streamwise wavenumber α and the amplitude function $\hat{\mathbf{q}}$ are allowed to vary rapidly in streamwise direction.

2.3 N-factor envelope

The n-factor, which measures the accumulated growth of the disturbances, is computed as $n(x) = \ln(A(x)/A_0)$, where A_0 denotes the maximum amplitude, in normal direction, of the streamwise velocity component of the corresponding TS mode at the streamwise position where the disturbance starts to grow. The n-factor is set to zero if during the course of the calculation, the value of A becomes smaller than A_0. Each n-factor curve is computed for a single TS wave defined by a particular nondimensional frequency F and spanwise wavenumber β. The nondimensional frequency F is defined as $F = 2\pi f^* \frac{\mu^*_\infty}{\rho^*_\infty (U^*_\infty)^2} \times 10^6$, where f^* is the physical frequency of the disturbances. The envelope of all n-factor curves considered is called the N-factor envelope, following the definition given by Arnal [7].

3 Numerical Results

3.1 Base Flow Computations

The laminar steady two-dimensional flow on a flat plate in the presence of a single step was computed numerically. We used the compressible Navier-Stokes solver TAU [8], developed at DLR. Grids were generated using the structured grid generator MEGACADS, also developed at DLR. A schematic representation of the computational domain and the boundary conditions imposed for computing the base flows is depicted in Fig. 1. Farfield boundary conditions were enforced sufficiently far from the surface irregularity (about 5000 δ^* in both streamwise and normal directions).

3.2 Base Flow Results

The base flow pressure $\bar{p}$ is made nondimensional by twice the incoming dynamic pressure, i.e. $\rho^*_\infty (U^*_\infty)^2$. Figure 3 shows the contours of $\bar{p}$ and streamlines for *large* steps. For FFS (Fig. 3-a),-c),-e)), the flow field remains attached for smooth steps, while for the rectangular-shaped case, a tiny recirculation area appears in front of the

step. For BFS (Fig. 3-b),-d),-f)), the parameter C has a crucial influence on the presence and size of the recirculation area. In particular, for very smooth steps ($C = 50$) the flow remains attached. If the shape parameter C is reduced (cases *BFS_H12_C10* and *BFS_H12_r*), a large bubble appears right after the step. The size of the bubble increases the more the shape of the step approaches the rectangular one.

In terms of pressure contours, it is interesting to notice that for BFS the pressure contours barely change with the shape of the step. However, for FFS the pressure gradients in the vicinity of the step become more intense as the step shape approaches that of a rectangular step.

3.3 Instability Analysis

The computation of the spatial development of a broadband spectrum of TS waves (each one computed individually as explained in Sect. 2.3) is described in this section. The spatial growth in amplitude of each TS wave is collected in the corresponding n-factor curve.

The instability analysis is performed in the domain $(x - x_c) \in [-500, 2000]$. An initial investigation done on a flat plate using PSE for several frequencies F and spanwise wavenumbers β revealed that two-dimensional ($\beta = 0$) TS waves of frequencies $F \in [20, 75]$ produce the highest n-factor curves in the domain mentioned above. When a surface irregularity is present, the multi-zonal approach described in Sect. 2.2 is applied. The interfaces between PSE and AHLNS are placed at $(x - x_c) = \pm 165$, sufficiently far away from the recirculation regions (see Fig. 3). The following results were obtained considering incoming two-dimensional TS waves ($\beta = 0$) with frequencies in the range $F \in [20, 75]$.

3.4 Effect of Step Height and Shape

3.4.1 Forward-Facing Steps

Figure 4 compares the N-factor envelope curves when *small* (-a)), *medium* (-c)) and *large* (-e)) FFS are considered. In the vicinity of the step, the development of the TS waves is driven by the pressure gradients that the presence of the step introduces into the flow field. It is well known (see Drazin and Reid [9]) that an acceleration in the flow usually has a stabilizing effect. Figure 5 shows the nondimensional pressure distribution at the wall $\bar{p}_{wall}$ when *small* (-a)), *medium* (-c)) and *large* (-e)) FFS are considered. The flat plate case is also included for comparison. For all cases, there is an initial deceleration of the flow (adverse pressure gradient) followed by a very rapid acceleration. This effect explains why in the step region $x \approx x_c$ there is a small increase in the N-factor curves followed by a reduction. The favorable pressure gradient around x_c increases with the height of the step, but it is also very

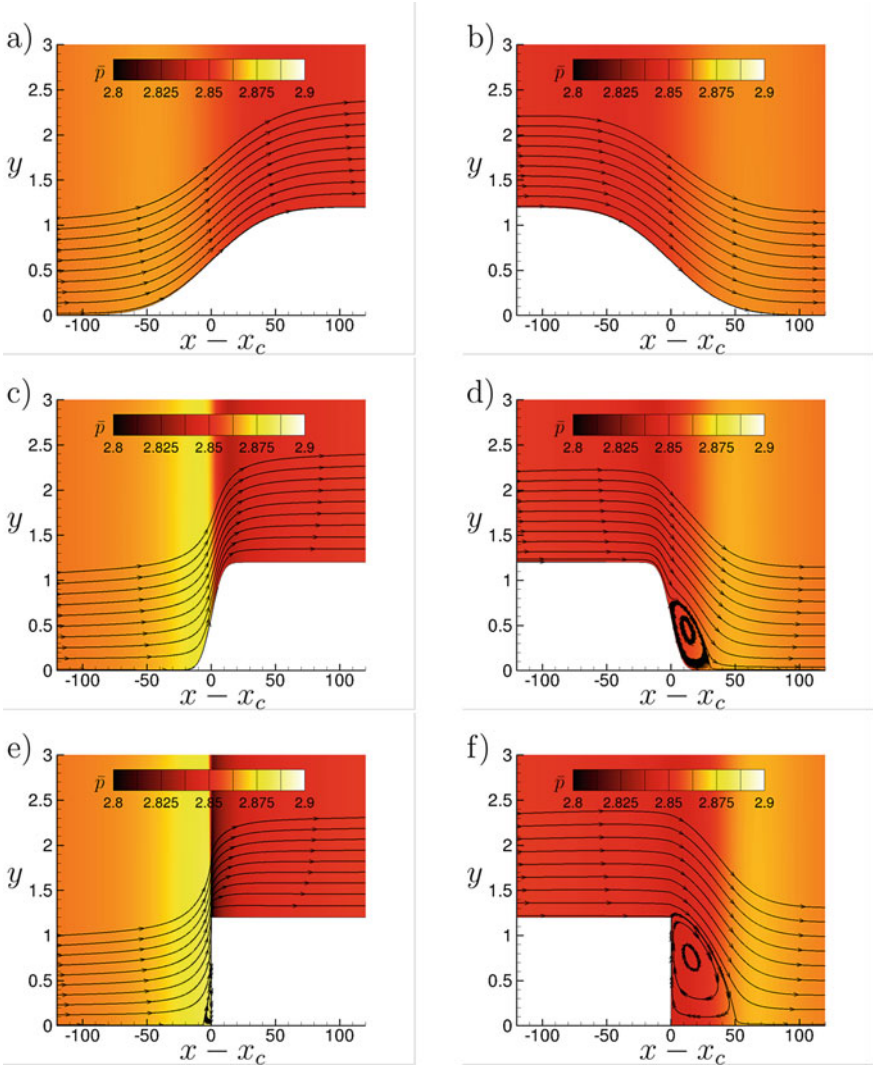

Fig. 3 Pressure $\bar{p}$ contours and streamlines for cases **a** *FFS_H12_C50*; **b** *BFS_H12_C50*; **c** *FFS_H12_C10*; **d** *BFS_H12_C10*; **e** *FFS_H12_r*; **f** *BFS_H12_r*. Flow direction is from left to right. Axes are not to scale

dependent on the shape of the step. Downstream, around $(x - x_c) \approx 50$, the pressure distribution starts to recover the ZPG, and the N-factor curves grow nearly parallel to the flat plate case.

3.4.2 Backward-Facing Steps

Figure 4 compares the N-factor envelope curves when *small* (-b)), *medium* (-d)) and *large* (-f)) BFS are considered. Similar to the above mentioned FFS, the development of the TS waves is driven by the pressure gradients that the presence of the step introduces into the flow field. Figure 5 shows the nondimensional pressure distribution at the wall $\bar{p}_{wall}$ when *small* (-b)), *medium* (-d)) and *large* (-f)) BFS are considered. For all cases, there is an initial acceleration of the flow (favorable pressure gradient) followed by a very rapid deceleration. This is the reason of the small reduction in the N-factor curves followed by a large increase in the vicinity of the step $x \approx x_c$. The adverse pressure gradient around x_c increases with the height of the step, but it is also very dependent on the shape of the step. Next, around $(x - x_c) \approx 50$, the pressure distribution starts to recover the ZPG, and the N-factor curves grow almost parallel to the flat plate case.

Although the pressure gradients around the step are less intense for BFS than for the corresponding FFS, the presence of a relatively large recirculation region, whose size depends strongly on the step shape as already described in Sect. 3.2, increases significantly the growth of the TS waves (see e.g. Hein [10]). Therefore, when a separation region is present in a BFS, the N-factors are considerably larger than for the FFS counterpart.

3.5 Prediction of Transition Location

The N-factor results of Fig. 4 can be used to assess the effects of the different surface irregularities on the transition location. Without having any further information, it is very common [11] to set the expected transition location x_{tr} as the closest point to the leading edge where the amplification curves reach the threshold value of $N_{tr} = 9$. The corresponding streamwise location is defined as the expected location where the transition to turbulence takes place. The resulting expected transition locations x_{tr} for the different cases are summarized in Fig. 6. In this figure, the expected transition location for a flat plate is named x_{tr_0}. The abscissa $(x_{tr}\text{-}x_c)/(x_{tr_0}\text{-}x_c)$ relates the downstream distance of the expected transition from the step position x_c to the downstream distance without any surface irregularity.

Costantini et al. [12] used the *loss of laminarity* Δs (%) as the counterpart of the parameter $(x_{tr}\text{-}x_c)/(x_{tr_0}\text{-}x_c)$. In this sense, the maximum Δs for *small* steps is about 14% (i.e. $(x_{tr}\text{-}x_c)/(x_{tr_0}\text{-}x_c) = 0.86$, case *BFS_H04_r*). However, for *large* steps the maximum Δs is about 94% (case *BFS_H12_r*), i.e. transition is expected to occur in the vicinity of the step. Interestingly, the effect of smoothing the step can reduce

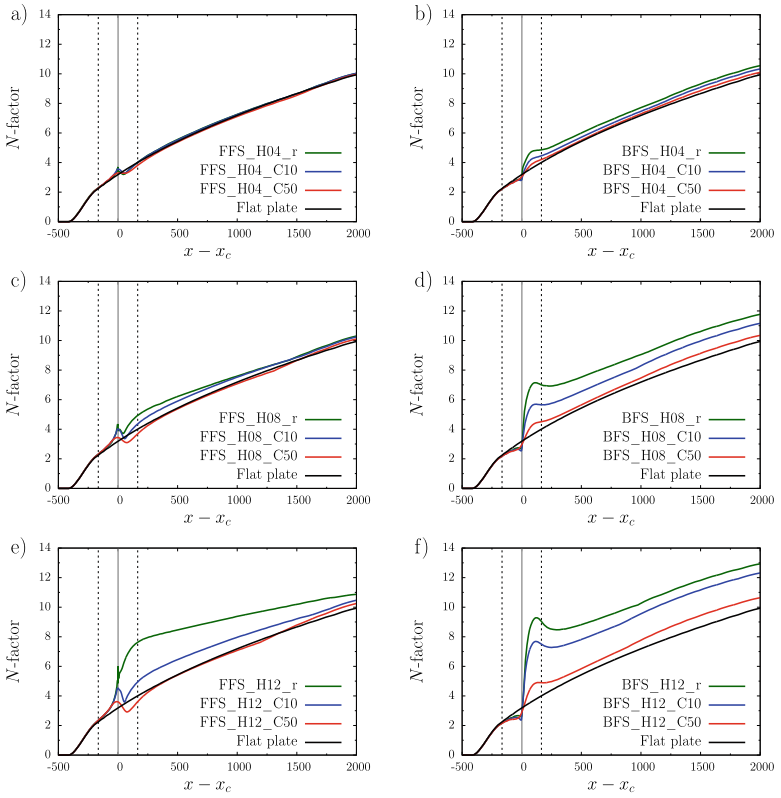

Fig. 4 Effect of shape parameter C on N-factor envelope curves for cases **a** *FFS_H04*; **b** *BFS_H04*; **c** *FFS_H08*; **d** *BFS_H08*; **e** *FFS_H12*; **f** *BFS_H12*. Vertical dashed lines indicate the location of the interfaces between PSE and AHLNS methodologies. The grey line represents the position of the step. The N-factor envelope curve for a flat plate (black line) is included as reference

the *loss of laminarity* up to only 17% (case *BFS_H12_C50*). Clearly, for *large* steps the impact of smoothing the shape of the step has a much stronger influence on the expected transition location. For *medium* steps the situation depends on the type of the step: for FFS the expected transition location is relative unaffected by the shape of the step, while for BFS the *loss of laminarity* can be reduced from 39% (case *BFS_H08_r*) to 10% (case *BFS_H08_C50*).

4 Summary and Conclusions

The spatial linear stability analysis of Tollmien-Schlichting waves in the presence of a large variety of forward- and backward-facing steps on a flat plate in a compressible flow is presented here. In order to reduce the scope of all possible parameter com-

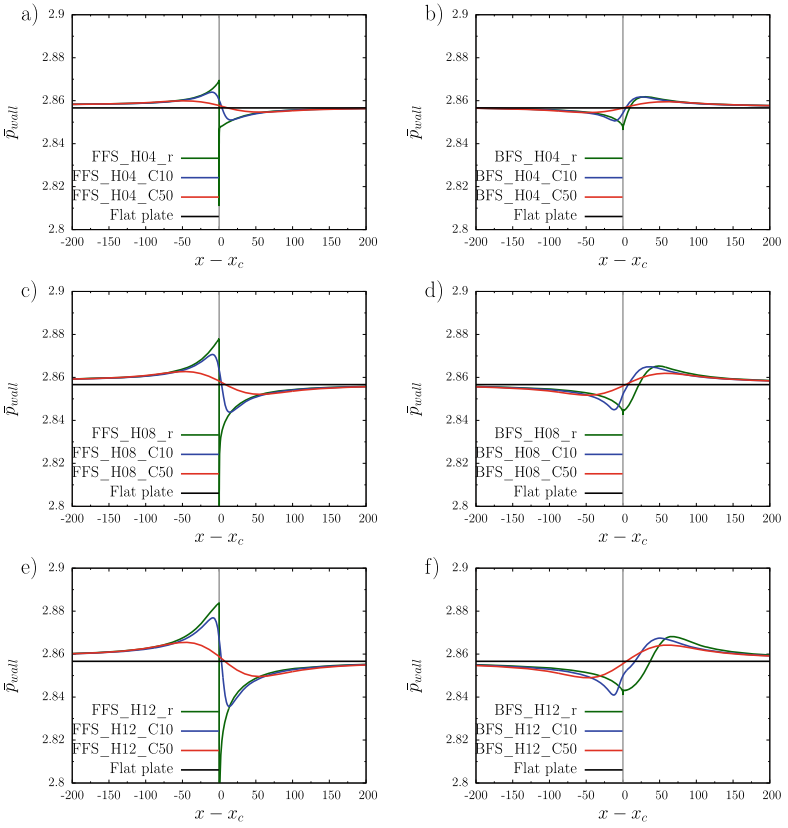

Fig. 5 Effect of shape parameter C on pressure distribution at the wall $\bar{p}_{wall}$ for cases **a** *FFS_H04*; **b** *BFS_H04*; **c** *FFS_H08*; **d** *BFS_H08*; **e** *FFS_H12*; **f** *BFS_H12*. The grey line represents the position of the step. The pressure distribution for a flat plate (black line) is included as reference

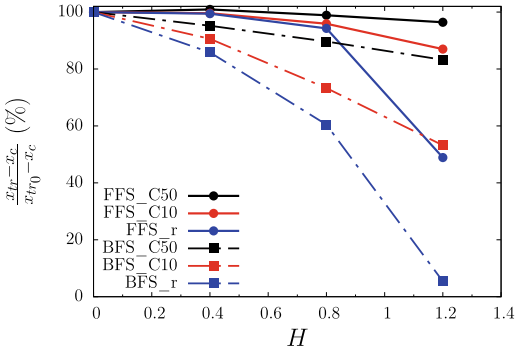

Fig. 6 Expected transition location x_{tr}, referred to the expected transition location for a flat plate x_{tr_0}, for all steps considered in the present work. The e^N methodology, with a transition N-factor of 9, is applied

binations, unit Reynolds number, Mach number and step location were kept fixed. The geometrical parameters which define the step (height and shape) were systematically varied. The recently developed AHLNS methodology was used to compute the N-factor envelope curve for each step.

A physical interpretation of the instability results, based on the changes in pressure distribution introduced by the presence of the step is also described in detail. The results of the stability analysis were related with an expected transition location via the e^N methodology, assuming that a value of N_{tr}=9 triggers the onset of transition to turbulence. It is shown that, for *small* steps (in terms of the displacement thickness at the step location x_c) the expected transition location is barely affected by the shape of the step (rounded or rectangular). However, for *large* steps the expected transition location for rectangular steps can be significantly delayed by smoothing the shape of the step. This effect was noticed for both forward- and backward-facing steps. However, further parametric studies which extend the scope of the present work are required in order to be able to describe completely all possible laminar-turbulent transition scenarios.

The AHLNS methodology presented here is very well suited for such parametric studies as it can be applied to other types of surface irregularities like humps, gaps, porous walls and suction slots, both in two-dimensional and quasi-three dimensional boundary layers. Quantifying the influence of such irregularities on the location of laminar-turbulent transition represents one of the major tasks in the design of laminar wings for future aircraft.

Acknowledgements Part of this work was supported by the European project NACOR (Grant Agreement no. CS2-AIR-GAM-2014-2015-01).

References

1. Nenni, J.P., Gluyas, G.L.: Aerodynamic design and analysis of an LFC surface. Astron. & Aeronaut. 52–57, (1966)
2. Ragab, S., Nayfeh, A.: Stability of compressible boundary layers over a smooth backward-facing step. AIAA Paper 1990–1449, (1990)
3. Edelmann, C.A.: Influence of forward-facing steps on laminar-turbulent transition. PhD Dissertation. Univ. Stuttgart (2014)
4. Franco, J.A., Hein, S., Valero, E.: On the influence of two-dimensional hump roughness on laminar-turbulent transition. Phys. Fluids. **32**, 034102 (2020)
5. Franco, J.A., Hein, S.: Adaptive Harmonic Linearized Navier-Stokes equations used for boundary-layer instability analysis in the presence of large streamwise gradients. AIAA Paper 2018–1548, (2018)
6. Hein, S., Bertolotti, F.P., Simen, M., Hanifi, A., Henningson, D.: Linear nonlocal instability analysis - the linear NOLOT code. DLR IB 223–94, A56 (1995)
7. Arnal, D.: Boundary layer transition: Predictions based on linear theory. In: Progress in Transition Modelling. AGARD report 793 (1994)
8. TAU-Code User Guide: DLR. v.2017.1.0. (2017)
9. Drazin, P.G., Reid, W.H.: Hydrodynamic Stability. Cambridge University Press (1981)
10. Hein, S.: Linear and nonlinear nonlocal instability analyses for two-dimensional laminar separation bubbles. Laminar-Turbulent Transition. Proceedings of the IUTAM Symposium (1999)

11. Masad, J.A., Iyer, V.: Transition prediction and control in subsonic flow over a hump. Phys. Fluids. **6**, 313–327 (1994)
12. Costantini, M., Risius, S., Klein, C.: Experimental investigation of the effect of forward-facing steps on boundary-layer transition. Procedia IUTAM. **14**, 152–162 (2015)